Accepted Manuscript

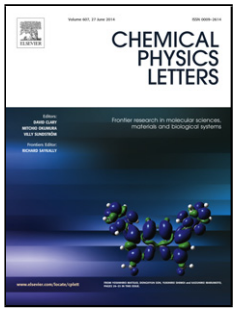

Title: A Characterization of the Two-step Reaction Mechanism of Phenol Decomposition by a Fenton Reaction

Author: Cristian Valdés Jans Alzate-Morales Edison Osorio Jorge Villaseñor Carlos Navarro-Retamal

PII: S0009-2614(15)00749-6
DOI: http://dx.doi.org/doi:10.1016/j.cplett.2015.10.005
Reference: CPLETT 33330

To appear in:

Received date: 2-7-2015
Revised date: 8-9-2015
Accepted date: 4-10-2015

Please cite this article as: C. Valdés, J. Alzate-Morales, E. Osorio, J. Villaseñor, C. Navarro-Retamal, A Characterization of the Two-step Reaction Mechanism of Phenol Decomposition by a Fenton Reaction, *Chem. Phys. Lett.* (2015), http://dx.doi.org/10.1016/j.cplett.2015.10.005

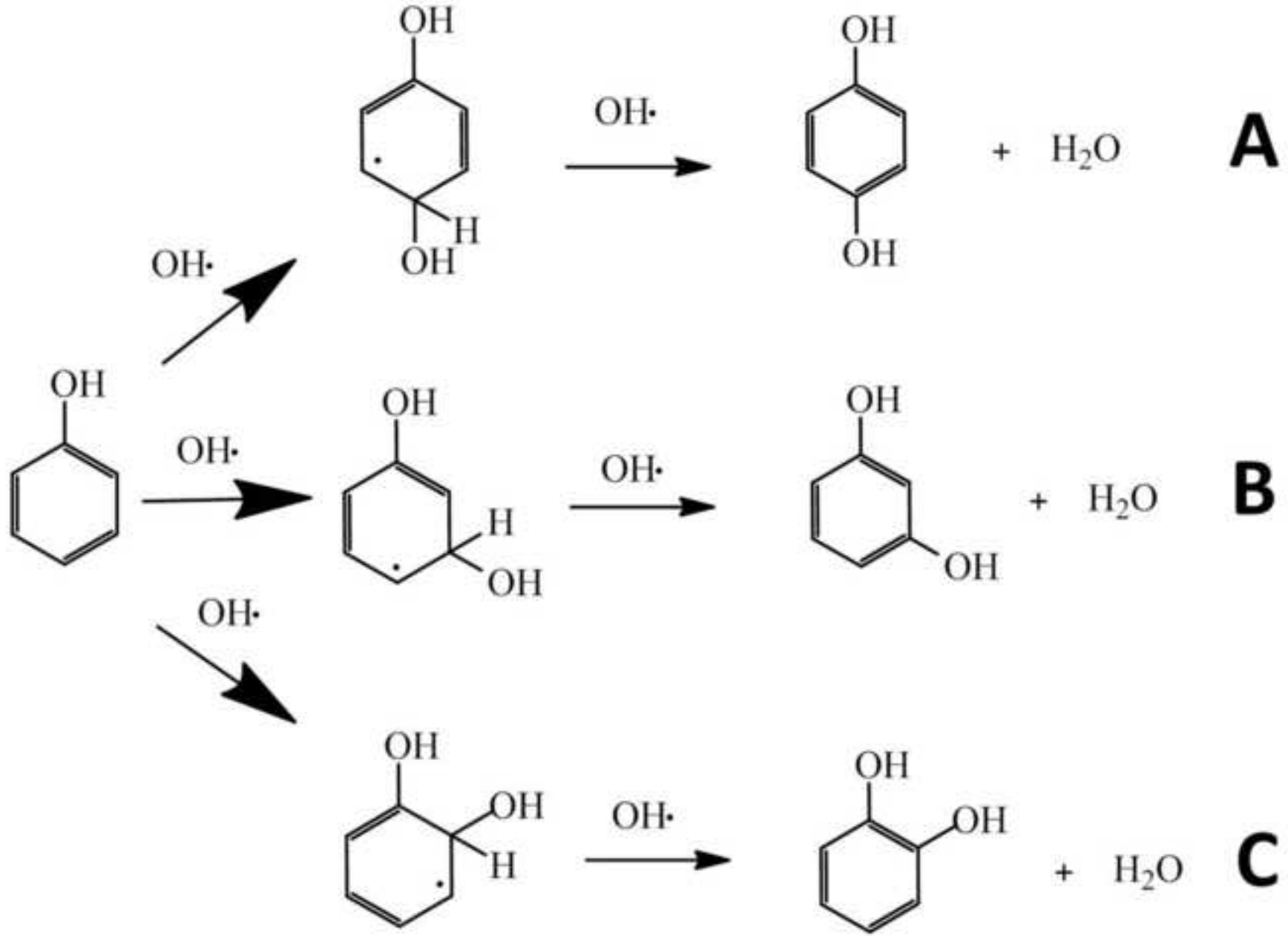
OH
OH·
OH
H
OH
OH·
OH
OH
+ H_2O
A
OH
OH·
OH
H
OH
OH·
OH
OH
+ H_2O
B
OH·
OH
OH
H
OH·
OH
OH
+ H_2O
C

Highlights

Oxidation of phenol (using Fenton) decrease in the presence of OH° scavengers.

The theoretical Ea of liquids systems are lower than gas phases.

Good agreement is found between DFT studies and experimental results.

Theoretical and experimental order shows the trend:
hydroquinone>catechol>resorcinol.

A Characterization of the Two-step Reaction Mechanism of Phenol Decomposition by a Fenton Reaction

*Cristian Valdés[2], Jans Alzate-Morales[1], Edison Osorio[3], Jorge Villaseñor[2, *] and Carlos Navarro-Retamal[1, *]*

[1] Centro de Bioinformática y Simulación Molecular, Facultad de Ingeniería, Universidad de Talca, 2 Norte 685, Casilla 721, Talca, Chile

[2] Laboratorio de Fisicoquímica, Instituto de Química y Recursos Naturales, Universidad de Talca, 2 Norte 685, Casilla 721, Talca, Chile

[3] Departamento de Ciencias Básicas, Fundación Universitaria Luis Amigó, Medellin, Colombia

AUTHOR EMAIL ADDRESS: cnavarro@utalca.cl and jvillase@utalca.cl

* CORRESPONDING AUTHORS FOOTNOTE:

C. Navarro-Retamal, Phone number: 56-71-201798, Fax number: 56-71-201561, Additional Email Address: carlos.navarro87@gmail.com

J. Villaseñor, Phone number: 56-71-2200272

ABSTRACT

Phenol is one of the worst contaminants at date, and its degradation has been a crucial task over years. Here, the decomposition process of phenol, in a Fenton reaction, is described. Using scavengers, it was observed that decomposition of phenol was mainly influenced by production of hydroxyl radicals. Experimental and theoretical activation energies (E_a) for phenol oxidation intermediates were calculated. According to these E_a, phenol decomposition is a two-step reaction mechanism mediated predominantly by hydroxyl radicals, producing a decomposition yield order given as hydroquinone > catechol > resorcinol. Furthermore, traces of reaction derived acids were detected by HPLC and GS-MS.

INTRODUCTION

Phenol is one of the most common contaminants ever known. This compound may come from the pharmaceutical industry, oil, pesticides and others. Lower amounts of phenol (in concentrations of ppm) are enough to induce high levels of toxicity [1]. Phenol is considered by the United States Protection Agency (USEPA) as one of the most pollutant compounds, causing considerable damage to human health and to the ecosystems [2]. The hydroxylation of phenol with oxidizing agents, like ozone and hydrogen peroxide, has a great impact on different fields such as environmental remediation and the photography industry (by using different phenol derivatives as photographic developers) [3].

The catalytic oxidation of phenol has proven to be really important along the last years, where different derivatives of this reaction, such as catechol (CT) and hydroquinone (HQ), can serve as raw materials for the generation of photographic supplies, pesticides,

inks and additives for medicines [4]. In order to improve the oxidation of this kind of molecules, many researches have used on the last decades a specific kind of oxidation process named advanced oxidation process (AOP), which usually operates at or near normal temperature and pressure conditions. According to Glaze *et al*., AOP is defined as a process that "involves the generation of hydroxyl (OH) radicals in sufficient quantity to affect water purification" [5]. OH radicals are extraordinarily reactive species. They are able to degrade the most part of organic compounds, with constant rates in the order of the 10^6 – 10^9 $M^{-1}s^{-1}$[6]. OH radicals are effective in destroying organic chemicals because they are reactive electrophiles that react rapidly and non-selectively with nearly all electron-rich organic compounds. It has been reported that one of the best source of OH radicals corresponds to the hydrogen peroxide (H_2O_2), because it has low cost, and more importantly, because is not harmful to the environment [7, 8]. On the other hand, the Fenton mechanism is based on the continuous production of radicals using the decomposition of H_2O_2 mediated by the ion Fe (II) as catalyst at pH 3 in a homogeneous system [9]. It is also known that phenol can be efficiently degraded by Fenton type processes [10]. Since Fenton processes are characterized by the generation of several radicals (i.e. $^{\bullet}OH$, $^{\bullet}O_2^-$ and $^{\bullet}O_2H$) [11, 12], the radical scavengers Chloroform (CF) and Isopropyl alcohol (IPA) were used in order to study its effect on the oxidation of phenol, considering their highly selectivity by superoxide (k=3,0 x 10^{10} M^{-1} S^{-1}) and hydroxyl radical (k=9,0 x 10^9 M^{-1} S^{-1}) respectively [9].

According to literature, three different intermediates are produced during the oxidation of phenol: catechol (CT), resorcinol (RC) and hydroquinone (HQ). Among them, HQ and CT are the most abundant, followed by RC [13]. It has been reported that other

radical species, such as superoxide radical, are also able to oxidase different aromatic compounds, including phenol [3, 14].

Some reaction mechanisms have been proposed to explain the oxidation of phenol mediated by H_2O_2 and OH radicals [15, 16]. For instance, the oxidation of phenol by OH radicals can be achieved by 3 different reaction mechanisms (Scheme 1). Each one consists in a two-step reaction, where the first step corresponds to the addition of an OH radical onto one of the carbons at the *ortho, metha* or *para* positions of phenol, leaving a delocalized electron on aromatic ring and thereby generating an adduct intermediate. The second step corresponds to the hydrogen abstraction (H-abst) at the same position of the previous addition, leading to the formation of a water molecule and the corresponding derivative. Depending on the carbon atom at which the second OH radical is added; three different intermediates can be produced. If both reactions occur at the *o*-carbon, the product will be CT (Scheme 1C); if instead both reactions occur at the *m*-carbon, the reactions will produce RC (Scheme 1B) and if the reactions occur at the *p*-carbon, the final product will be HQ (Scheme 1A). Furthermore were detected by HPLC and GS- MS: traces of maloneic, malic, pyruvic and acetic acids among others (data not shown).

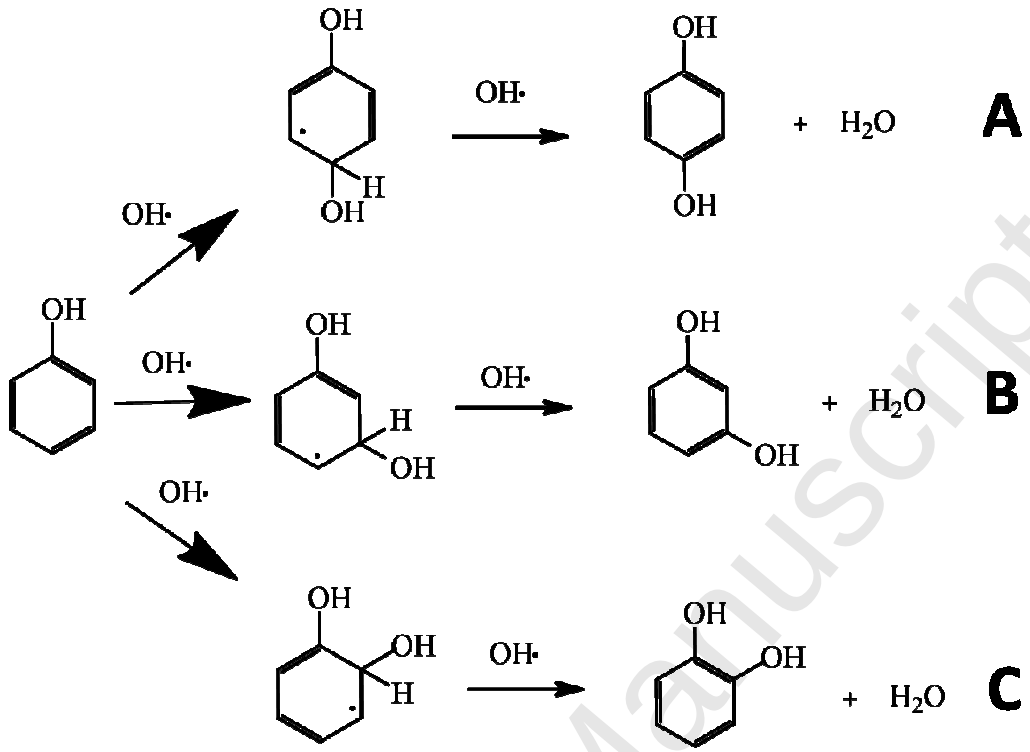

Scheme 1. Reaction mechanism describing the different phenol intermediates based on the interaction of phenol with two hydroxyl radicals. A) Generation of HQ by the interaction of the hydroxyl radicals onto the *p*-carbon of phenol. B) Generation of RC by the interaction of the hydroxyl radicals onto the *m*-carbon of phenol. C) Generation of CT by the interaction of the hydroxyl radicals onto the *o*-carbon of phenol.

Until date, the addition step has been scarcely described at a theoretical level. For instance, Wu *et al*. described the addition step of the OH radical on gas phase in 4 possible positions at phenol ring: *ipso, ortho, meta* and *para* of phenol. They found that addition at the *o*-carbon was thermodynamically favorable, resulting in an overall production of 96.7-99.8% of the total adduct products in the reaction [17]. In a similar way, Morales-Roque *et al*. were able to study the same step, but now including the solvent effects onto the overall system. They found that adducts at *o*- and *p*-carbons were the chemical entities that showed the lower energy barriers, thereby producing a bigger amount of *o*-adducts and *p*-adducts [8]. At date, there is not theoretical evidence

related to the second step of the reaction mechanism, neither in gas phase or water as a solvent.

In this research work, the main goal is twofold: first, to experimentally elucidate the importance of the OH radical during phenol decomposition; and second, to characterize the two-step decomposition reaction mechanism pathway of phenol by means of theoretical approaches. The research involves the theoretical study of the solvent effect into this kind of reaction.

METHODOLOGY

Quantification of Phenol and its intermediates by HPLC

The concentration of phenol was analyzed using a HPLC (Perkin Elmer series 200) equipment with a LiChrospher® column RP-18 with UV absorbance detector. The following conditions were used: λ=280 nm, flow = 1 mL / min, mobile phase methanol (34%) / water (64%) / acetic acid (2%), column at temperature 35° C with an injection volume of 10 μL.

The concentration of phenol intermediates was analyzed using a HPLC (Perkin Elmer series 200) equipment with a LiChrospher® column 60 RP Select B coupled to a Shimadzu Prominence RF-20-A / 20AXS fluorescence detector. The following conditions were used: λ emission = 325, λ excitation = 280, flow of 1 mL / min, mobile phase 0.007 M H_3PO_4 (90%), acetonitrile (10%), column temperature at 45 °C, with an injection volume of 10 μL.

Phenol and its intermediates concentrations were determined using calibration curves obtained from solutions of known concentration for each case.

The solutions were prepared in triplicate and transferred to the autosampler microvials and samples of 200 μL were injected into the column. Calibration curves were constructed by plotting the peak area against the nominal concentration of each compound.

Five samples of each compound were prepared at the quality control in four different concentrations, in three different days, in order to determine intra- and inter-day precision and accuracy.

The acceptance criteria for the limit of quantification was that the accuracy for three analyzed samples presented less than 2 % variability and the limit of detection was measured taking into account a signal-to-noise ratio of three.

Radical mediated phenol decomposition in the presence of isopropyl alcohol (IPA) and chloroform (CF) as scavengers

Radical mediated decomposition of phenol was achieved using an Advanced Oxidation Process (AOP) methodology, which is based in the application of Fenton reaction mechanism. In order to verify the effect of radicals, some scavenger molecules like isopropyl alcohol (IPA) and chloroform (CF) were used.

The system components, Fenton-Phenol-scavenger, were mixed by a continuous stirring in the next concentrations: phenol 50 ppm (Fluka), H_2O_2 (Merck), 1 mM, $Fe(SO_4) \cdot 7H_2O$ (as source of Fe (II) ions) (Merck), 0,5 g/L and 250 mM of IPA (Sigma Aldrich) or 2 mM of CF (Merck), depending on each case. All the reaction assays were performed at 25ºC, pH 3 in a total volume of 50 mL of water. Fenton reaction was stopped at basic pH using a phosphate buffer at pH 8 [18].

Experimental determination of Activation energy

In order to measure the activation energy for phenol decomposition into the different intermediates HQ, CT and RC, the components Fenton-Phenol were mixed by a continuous stirring using phenol 50 ppm (Fluka), H_2O_2 (Merck) 1 mM and $Fe(SO_4) \cdot 7H_2O$ (Merck) 0,5 g/L. All the assays were performed at pH 3 in a total volume of 100 mL of water, the reactions were stopped after one minute using a phosphate buffer at pH 8 and then they were analyzed by HPLC. The experiment was performed at different temperatures (5, 15, 25, 35 and 45 °C).

In order to estimate the activation energies, the initial velocities method was used, where *Ea* was measured by the Arrhenius equation as follows:

$$Log\ V_0 = Log\ A - \frac{Ea}{RT} \qquad \text{(Equation 1)}$$

Where *R* is the ideal gas constant, *T* is the absolute experimental temperature and *Ea* is the activation energy, A is a constant and V_0 is the initial velocity of the reaction [19].

Computational Studies on Phenol and its byproducts

Phenol local reactivity

In order to determine the reactivity of phenol, local theoretical descriptors in the framework of density functional theory (DFT) were used [20, 21]. The Fukui function (adjusted to radicals) was used according to the following equation[22]:

$$f^0\vec{r} = \frac{(\rho_{N+1}(\vec{r}) - \rho_{N-1}(\vec{r}))}{2} \qquad \text{(Equation 2)}$$

Where $\rho_{N+1}(\vec{r})$ corresponds to the electron density of the N-electron species when the system gains an electron (anion), and $\rho_{N-1}(\vec{r})$ when it loses an electron (cation). In order to obtain the electron density for a given region at the molecule, it is necessary to divide the molecular space with subsequent integration of the Fukui function on those regions. To do so, Tiznado *et al.* proposed a methodology to condense the Fukui function to regions using the following expression [23, 24]:

$$f_k^0 = \int_{w_k} f_k^0(\vec{r})\overrightarrow{dr} \qquad \text{(Equation 3)}$$

Where the ω_k region is obtained from the topological analysis of the Fukui function, and f_k^0 is the condensed value of the Fukui function in that specific region [25].

All calculations were performed with the B3LYP [26, 27] method using the 6-311+(d, p) basis set [28] as available in Gaussian 09 electronic structure software [28-30].

Characterization of Transition States for Phenol Decomposition Reactions

Transition state search was performed at an unrestricted DFT level of theory [31] using the LST (Linear Synchronous Transit) method. All geometries (reactants, transition states and products structures) were fully optimized at the B3LYP/6-31G (d) [26, 27] level of theory. By performing frequencies analysis, the character of each stationary point was evaluated, which means that geometries with only positive frequencies (eigenvalues) correspond to a minimum and geometries with only one imaginary frequency should correspond to a transition state geometry. The motion of the main vibrational mode corresponded to the desire reaction pathway. The solvents effects were

introduced by a polarizable continuum model (PCM) based on both, the solute and its electron density and the solvent as a continuum dielectric medium [32].

To check if the transition states were properly located, an intrinsic reaction coordinate algorithm (IRC) was used [33] that is defined as the steepest descent (SD) curves connecting a first-order saddle point (the transition structure) with a minimum, which is characteristic of a stationary point (corresponding to either reactants or products). IRC parameters used were: MaxPoints = 80, maxcycle = 300 and stepsize = 2.

RESULTS AND DISCUSSION

Decomposition of phenol mediated by OH radicals

With the aim to show that decomposition of phenol by AOP process, using H_2O_2 and Fe (II) ions in a Fenton reaction, is dependent on the OH radical concentration; the phenol decomposition was measured in presence of two scavengers: Isopropyl alcohol (IPA) and chloroform (CF). IPA is specific for hydroxyl radicals ($OH^{\bullet}$) while CF is specific for superoxide radical ($O_2^{-\bullet}$).

Phenol decomposition was measured in three different times (10, 20 and 30 minutes) at 25 ºC and using 6 different experimental conditions: a) Only H_2O_2 (unmediated by radicals), b) H_2O_2 + IPA, c) H_2O_2 + CF, d) Fenton, e) Fenton + IPA and f) Fenton + CF (see Figure 1). Overall, it was found that phenol decomposition by H_2O_2 barely reached the 12% at 30'. When scavengers were added, there was only a 2% decrease in phenol decomposition at 30' using IPA and less of 1% using CF, suggesting that H_2O_2 is unable to spontaneously decompose on radical species, which may explain the overall low decomposition of phenol under those initial experimental conditions. By using a Fenton

system, it was found that overall decomposition of phenol increases significantly at different measuring times, reaching about 30% in the first 10 minutes. Since it is well known that catalysts based in transition metals are able to accelerate the decomposition of H_2O_2 into radical species [9, 34], this last result confirmed that radicals are the mainly species involved in decomposition process of phenol. When IPA and CF scavengers were added into experiment **d)** (H_2O_2 + Fe (II), Fenton), two phenomena could be observed: By adding CF, the overall phenol decomposition process did not show a marked decrease in the percentage of inhibition (barely 2%), which roughly means that the superoxide radical could not be responsible of the phenol decomposition process. On the other hand by adding IPA as scavenger, and comparing experiments **d** and **e**, it is observed that the yield of decomposition is decreased about 3 times at all measured times, which could indicate that the OH radical is the key chemical specie that drives the phenol decomposition process. The effect of CF in phenol decomposition (experiment **f**) was lower only about 6% when compared with experiment **d**, which could indicate that the effect of superoxide radical in these conditions is not relevant compared to the hydroxyl radical.

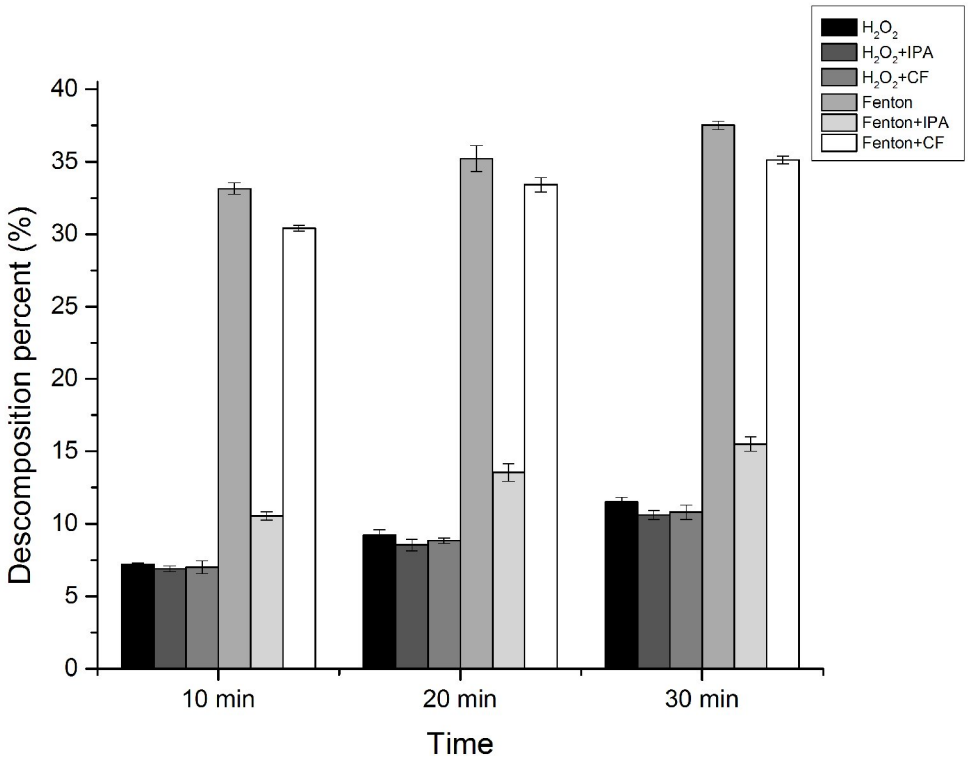

Figure 1. Bars representation of phenol decomposition percentages measured at different times and using several experimental conditions.

Phenol decomposition and characterization of its intermediates

The concentrations (in ppm) of three different intermediates (CT, RC and HQ), from H_2O_2 induced phenol decomposition, were measured during time at two different conditions: in presence and absence of Fenton reactant, now on called F and wF, respectively. The experiments were carried out at 25º C and pH 3 (Figure 2). It was found that HQ is the main intermediate produced in the experimental degradation assays, and moreover its production was enhanced by the presence of Fenton reactant (more than two times with respect to the non catalytic process). The other main

products determined in phenol degradation reactions were CT and RC, which is in agreement with previous literature [35]. It is important to note that the amount of HQ produced is about 5 times greater than RC, both in presence and absence of the Fenton system. The amount of CT is produced 3 to 4 times greater than RC in the presence of Fenton system.

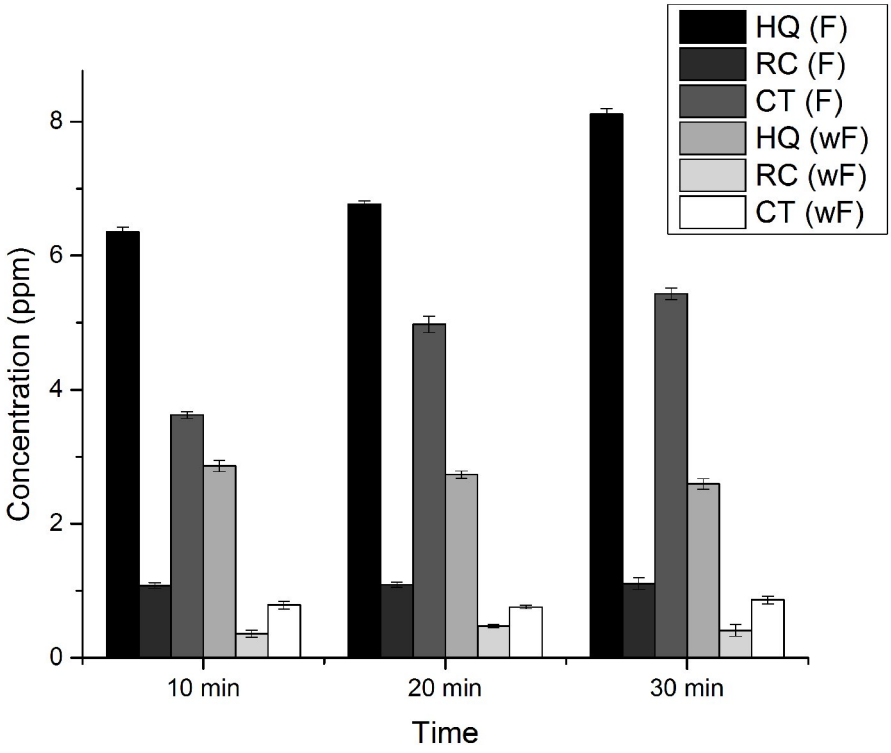

Figure 2. Concentration (in ppm) of intermediates CT, RC and HQ during induced decomposition of phenol. The experiments were carried out in presence (F) and absence (wF) of Fenton process

Experimental determination of Activation energies

In order to explain the differences in the amount of each intermediate produced during the decomposition of phenol, the activation energy (E_a) for each reaction was measured.

Using different residence times and temperatures, E_a was estimated for the three reaction mechanisms (Scheme 1) based on the slopes calculated from plots reported in Supplementary Material (Figure 1S, Figure 2S and Figure 3S). It was found that the production of RC presented the highest E_a with a value of 2,534 kcal/mol. On the other hand, the production of CT and HQ exhibited lower activation energies (1,174 and 0,855 kcal/mol, respectively).

These E_a differences could be explained by the electron density properties of phenol, which indicates that its *m*-carbon presents a lower electron density while the *o*-carbon and *p*-carbon present a higher electron density. It has been reported the appearance of HQ and CT in electrochemical oxidation processes of phenol, and moreover these two intermediates were detected in phenol oxidation processes in the presence of hydrogen peroxide and acetone [13, 36].

DFT Reactivity Indexes Analysis

As a previous step, before the theoretical characterization of the reaction mechanisms of phenol decomposition, the electron density of phenol was studied by measuring its Fukui local indexes for a radical reaction.

According to the radical Fukui index (FI) analysis (Figure 3 and Table 1), it was found that *o*- and *p*-carbons are more susceptible to a radical attack, by the first hydroxyl radical, than the *m*-carbon (FI values: *ortho* = 0.0387-0.0387 *meta* = 0.0251-0.0249 and *para* = 0.1241). It is worth mentioning that this type of method is useful to find regioselectivity of molecules against radicals, but it does not discriminate the type of

radical. We found that, according to FI, the most favored intermediaries are hydroquinone (*para*) and catechol (*meta*).

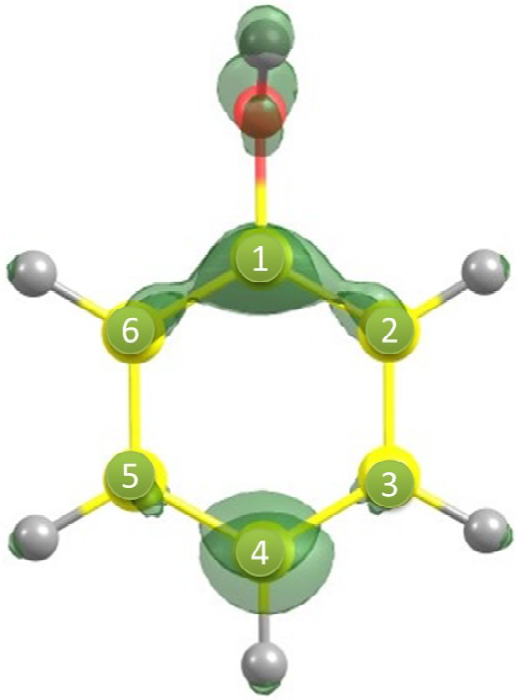

Figure 3. Ball and sticks representation of phenol molecule that represents its Fukui local indexes at each numbered carbon atom (according to Table 1). In yellow, red and grey are represented the carbons, oxygen and hydrogen atoms, respectively. The electron density obtained by the Fukui analysis is represented on green.

Table 1. Carbon atoms in phenol molecule and their radical Fukui index values.

Carbon atom	Fukui index (FI)
1	0,0848
2	0.0387

3	0.0251
4	0.1241
5	0.0249
6	0.0387

Characterization of transition states geometries and phenol decomposition reaction paths.

A single imaginary frequency (lower than -90 cm^{-1}) was found for each of the transition state species calculated both in gas or solvent phase (see Table S1).

OH radical addition as first reaction step

The oxidation of phenol molecules is mediated by a two-step reaction mechanism, which comprises the attack of electrophilic radicals (OH radicals) at three different positions in the phenolic ring. While the first step has been described both on gas and solvent [8, 17], to the best of our knowledge, there are not theoretical studies related to the hydrogen abstraction step neither in gas or solvent phase.

The reactants, TSs and products structures, as well as their corresponding activation energies, for the first reaction step in each possible phenol decomposition reaction are presented in Figures 4 and 5, for gas and solvent phase, respectively. The oxygen atom, belonging to the hydroxyl radical, was located around 2.02 – 2.05 Å with respect to the corresponding carbon atom (position *ortho, meta* and *para*) in each TS structure (Table S2 and S3). The addition of the first OH radical (on the 3 different systems) showed an energy barrier from 0,504 to 1,573 kcal/mol. According to previous reports, some reactions between phenols and electrophilic compounds are in the order of the 4

kcal/mol [8, 17, 37]. Based on those results, the first reaction step that showed the lowest E_a in decomposition of phenol is favored on the *p*-carbon, which in turn is in agreement with our experimental data that reported more production of the HQ intermediate. The E_a values for CT and RC decomposition products are higher in energy and, thereby, their production would be disfavored.

Gas phase (step 1)	Reactants	TS	Products (radical species)
Para	 0 kcal/mol	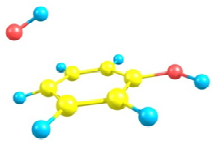 0,504 kcal/mol	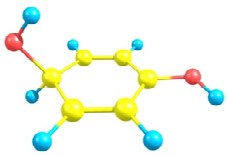 -14,981 kcal/mol
Ortho	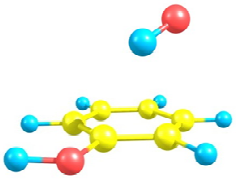 0 kcal/mol	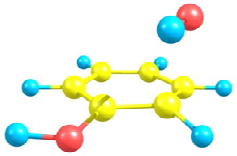 1,573 kcal/mol	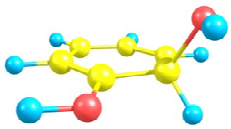 -15,451 kcal/mol
Meta	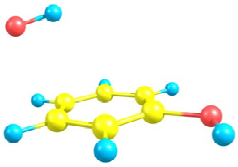 0 kcal/mol	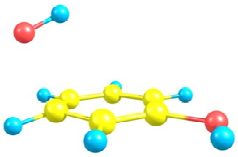 1,771 kcal/mol	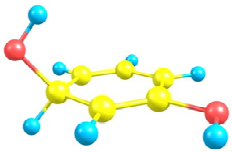 -14,244 kcal/mol

Figure 4: Reactants, TSs and products structures for step 1 in the gas phase, with their relative energies, are shown. Atom types are: Carbon (yellow), oxygen (red) and hydrogen (cyan).

Solvent phase (step 1)	Reactants	TS	Products (radical species)
Para	 0 kcal/mol	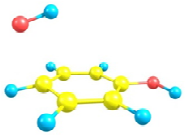 0,0201 kcal/mol	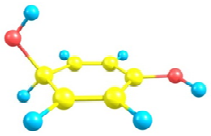 -12,4250 kcal/mol
Ortho	 0 kcal/mol	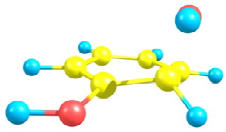 0,4118 kcal/mol	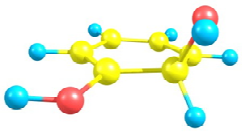 -13,1074 kcal/mol
Meta	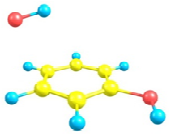 0 kcal/mol	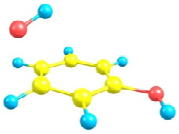 1,7055 kcal/mol	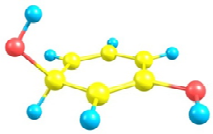 -11,5014 kcal/mol

Figure 5: Reactants, TSs and products structures for step 1 in solvent phase, with their relative energies, are shown. Atom types are: Carbon (yellow), oxygen (red) and hydrogen (cyan).

Hydrogen Abstraction, mediated by OH radicals, as the second reaction step

With respect to the second reaction step, the transition state geometries showed that a second OH radical was located at 2.37 – 2.41 Å with respect to the carbon atom at the corresponding position in phenol ring. The oxygen atom from OH radical was located at a distance between 1.30 – 1.34 Å with respect to the leaving hydrogen atom (see Table S1 in Supplementary Information). According to IRC energy profiles for second reaction step in gas phase, that means the leaving of H atom mediated by a second OH radical (Figures 6 and 7), it was found that phenol decomposition reaction that showed

the highest E_a values corresponds to the H-abst onto the *m*-carbon that produces RC (25.893 kcal/mol), followed by the reaction occurring onto the *p*-carbon (22.137 kcal/mol) that produces HQ and finally by the reaction occurring onto the *o*-carbon (19.131 kcal/mol) that produces CT. Those calculated E_a values are not in fully agreement with our experiments, however they could explain the fact that the intermediate RC showed the lowest concentration during the phenol decomposition reaction studied through our experiments. In order to fully understand the correct reactivity trends in the production of RC, CT and HQ intermediates, subsequent estimation of IRCs including the solvation effect were performed.

Since this second reaction step occurs on water, the E_a values were also estimated in presence of a continuum dielectric field that represents an implicit water solvent. With respect to the OH addition, the final transition state structures showed distances, between the OH radical oxygen atom and the carbon atom in phenol ring, ranging from 2.01 to 2.12 Å (Table S1). When comparing the E_a values for this first reaction step calculated in implicit solvent, against those obtained in gas phase, it can be seen that they decreased for all three reactions in the presence of water as solvent. This phenomenon could be explained by the fact that in organic reactions the electrostatic component of the solvent acts as a catalyst reducing the energetic barrier of the reaction [38] even in the case of reactions that involves free-radicals [39]. It has been reported that E_a is affected by the degree of polarity of the solvent in reactions of polymerization [40] and polar organic solvents tend to decrease E_a in enzymatic systems [41].

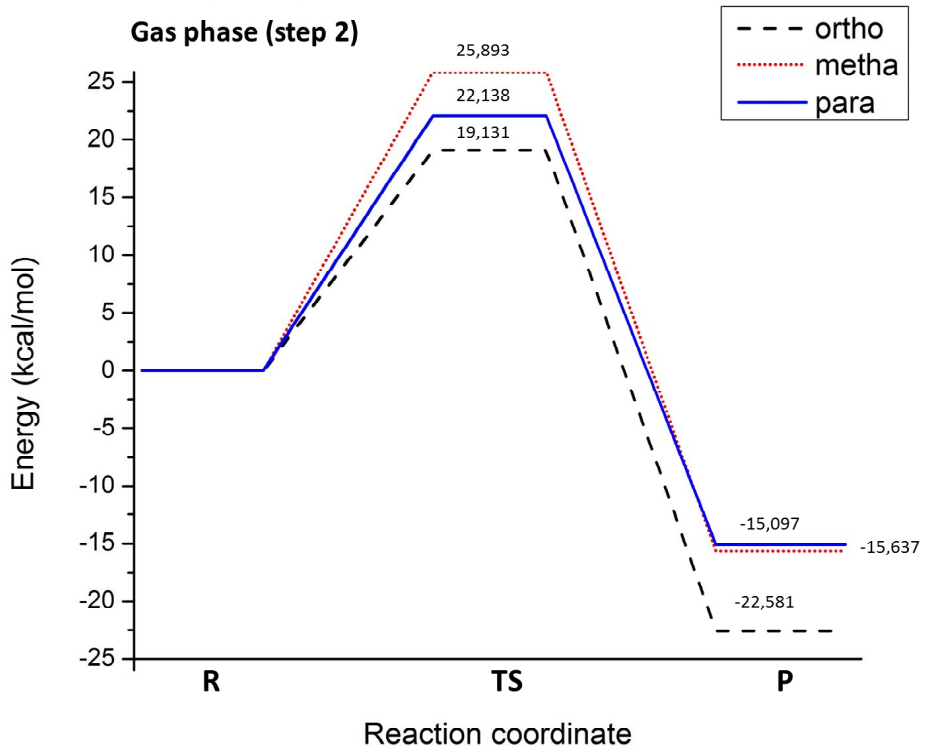

Figure 6: IRC profile with relative energies representing the second step intermediates, in the oxidation of phenol, calculated in gas phase. R (Reactant), TS (Transition State), P (Product).

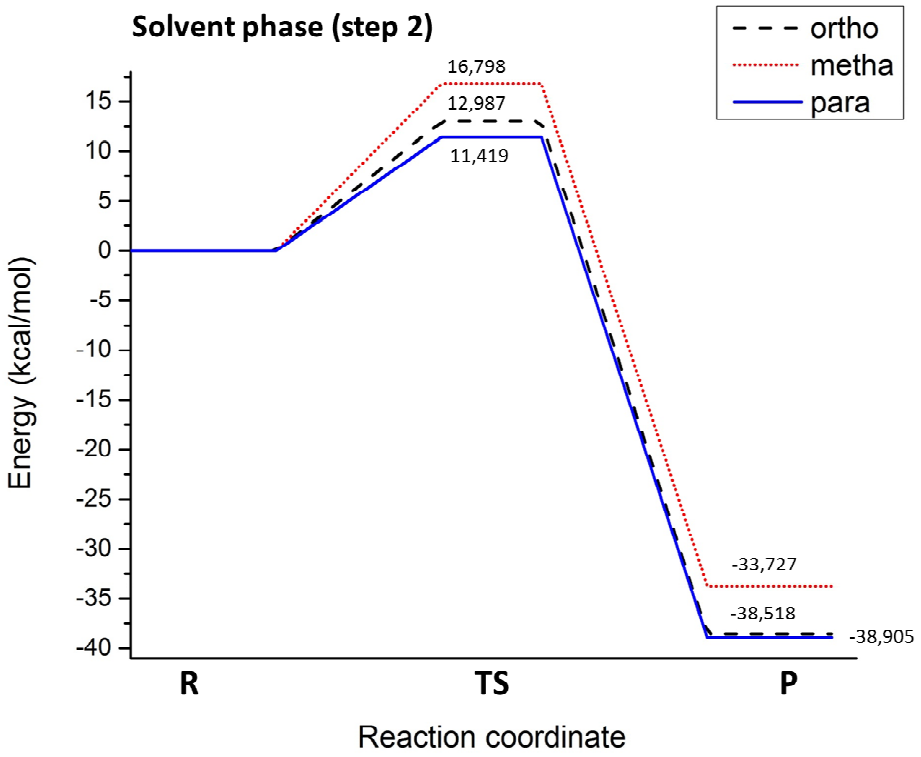

Figure 7: IRC profile with relative energies representing the second step intermediates, in the oxidation of phenol, calculated in solvent phase. R (Reactant), TS (Transition State), P (Product).

Regarding to the H-abst, the transition state structures showed distances, between the OH radical oxygen and the carbon atom, that were between 2.06 – 2.63 Å. Likewise, the distances between the OH radical oxygen and the leaving hydrogen atom showed values between 1.55 – 1.74 Å (Table S3).

The calculated E_a values for H-abst in solvent, when compared with their counterpart values in gas phase systems, showed a marked decrease in all cases (for instance a marked decrease of ~11 kcal/mol could be seen in the case of the H-abst onto the *p*-carbon), This seems reasonable due to the fact that all these kind of reactions occurs, and are favored, on water [25, 26]. Then, the determined solvent E_a values for the

reaction giving RC as product confirmed us that its low production could be due to the high-energy barrier of the process. With respect to the other phenol derivatives, it was observed that in presence of the electrostatic component of the solvent, the E_a values for production of HQ were lower than the ones for CT (11.42 and 12.99 kcal/mol, respectively) indicating now the correct trend found in our experimental results, that is: during phenol oxidation HQ is the most abundant phenol derivative, followed by CT and finally RC (that is barely produced *in vitro*).

CONCLUSIONS

The decomposition of phenol, by using the oxidizing agent hydrogen peroxide, was studied using HPLC and DFT approaches. It was found that decomposition increased about 5 times in the presence of Fe (II) in a homogeneous Fenton system. Thus, decomposition of phenol in these conditions seems to be highly dependent on hydroxyl radicals, because in the presence of scavenger IPA the performance of reaction decreases to the half when using catalyst. Regarding the use of CF as scavenger, the effect in lowering the performance of decomposition reaction is subtle. So, we suggest that primarily hydroxyl radicals would carry out the decomposition of phenol in the studied conditions. Generating a high amount of hydroxyl radicals permits efficient decomposition of a variety of harmful substances because it is one of the strongest oxidizing described [42, 43]. Further analysis are required to validate our hypothesis (i.e spin radical experiments), but we believe that our protocol suggest an implication of hydroxil radicals on phenol decomposition.

On the other hand, the two-step phenol decomposition reaction mediated by OH radicals was successfully described by both theoretical and experimental studies. According to our experimental approach, HQ was the derivate produced in larger quantities, followed by CT and finally RC. From the *in silico* approach, it was found that the activation energy profile for each reaction, estimated on a continuum solvation model, showed the same trend. Finally, from experimental and theoretical approaches, it was possible to determine that during this phenol decomposition reaction mechanism, the intermediates HQ and CT were the main decomposition products, which is in agreement with previous reported studies. The HPLC method proved highly efficient for quantifying phenol and related compounds, in addition to the use of a fluorescence detector that had a high sensitivity for products generated even in concentrations of parts per billion.

To the best of our knowledge, there are no previous reports of a theoretical characterization, through IRC method, of intermediates participating in the second step of phenol oxidation mechanism mediated by hydroxyl radicals.

ACKNOWLEDGMENT

The authors thank to "Centro de Bioinformática y Simulación Molecular" at Universidad de Talca for providing the computational time and resources to successfully accomplish all computational simulations reported in this work. C.N-R thanks Government of Chile for a doctoral fellowship awarded through CONICYT Nº 21120691. C.V. thanks Universidad de Talca and Pacific Chemical for a doctoral fellowship through the Applied Sciences Ph.D. program.

REFERENCES

1. Yang, et al., *Degradation of high concentration phenol by ozonation in combination with ultrasonic irradiation.* 2010. 21(1-3): p. 9.
2. Suranjana, C. and B.K. G, *Catalytic wet oxidation of phenol and its derivatives with Fe2O3 and MnO2.* Indian journal of chemical technology, 2006. 13(5): p. 499-504.
3. Park, J.-N., et al., *Hydroxylation of phenol with H2O2 over Fe2+ and/or Co2+ ion-exchanged NaY catalyst in the fixed-bed flow reactor.* Journal of Molecular Catalysis A: Chemical, 2006. 247(1-2): p. 73-79.
4. Qiao, J.-Q., et al., *Determination of catalytic oxidation products of phenol by RP-HPLC.* Research on Chemical Intermediates, 2012. 38(2): p. 549-558.
5. Glaze, W.H., J.-W. Kang, and D.H. Chapin, *The Chemistry of Water Treatment Processes Involving Ozone, Hydrogen Peroxide and Ultraviolet Radiation.* Ozone: Science & Engineering, 1987. 9(4): p. 335-352.
6. Cater, S.R., et al., *UV/H2O2 Treatment of Methyl tert-Butyl Ether in Contaminated Waters.* Environmental Science & Technology, 2000. 34(4): p. 659-662.
7. El-Hamshary, H., M.H. El-Newehy, and S.S. Al-Deyab, *Oxidation of Phenol by Hydrogen Peroxide Catalyzed by Metal-Containing Poly(amidoxime) Grafted Starch.* Molecules, 2011. 16(12): p. 9900-11.
8. Morales-Roque, J., et al., *Theoretical and experimental interpretations of phenol oxidation by the hydroxyl radical.* Journal of Molecular Structure: THEOCHEM, 2009. 910(1–3): p. 74-79.
9. Hwang, S., S.G. Huling, and S. Ko, *Fenton-like degradation of MTBE: Effects of iron counter anion and radical scavengers.* Chemosphere, 2010. 78(5): p. 563-568.
10. Babuponnusami, A. and K. Muthukumar, *Advanced oxidation of phenol: A comparison between Fenton, electro-Fenton, sono-electro-Fenton and photo-electro-Fenton processes.* Chemical Engineering Journal, 2012. 183(0): p. 1-9.
11. Pignatello, J.J., D. Liu, and P. Huston, *Evidence for an Additional Oxidant in the Photoassisted Fenton Reaction.* Environmental Science & Technology, 1999. 33(11): p. 1832-1839.
12. Halliwell, B., *Superoxide-dependent formation of hydroxyl radicals in the presence of iron salts is a feasible source of hydroxy radicals in vivo*. Vol. 205. 1982. 461-3.
13. Enache, T.A. and A.M. Oliveira-Brett, *Phenol and para-substituted phenols electrochemical oxidation pathways.* Journal of Electroanalytical Chemistry, 2011. 655(1): p. 9-16.
14. Lee, S., J. Oh, and Y. Park, *Degradation of phenol with fenton-like treatment by using heterogeneous catalyst (modified iron oxide) and hydrogen peroxide*. Vol. 27. 2006, Seoul, COREE, REPUBLIQUE DE: Korean Chemical Society. 6.

15. He, Y.Z., W.G. Mallard, and W. Tsang, *Kinetics of hydrogen and hydroxyl radical attack on phenol at high temperatures.* The Journal of Physical Chemistry, 1988. 92(8): p. 2196-2201.
16. Xu, C. and L. Wang, *Atmospheric Oxidation Mechanism of Phenol Initiated by OH Radical.* The Journal of Physical Chemistry A, 2013. 117(11): p. 2358-2364.
17. Wu, P., et al., *Theoretical study of mechanism and kinetics for the addition of hydroxyl radical to phenol.* Science China Chemistry, 2012. 55(2): p. 270-276.
18. Wink, D.A., et al., *The Fenton oxidation mechanism: reactivities of biologically relevant substrates with two oxidizing intermediates differ from those predicted for the hydroxyl radical.* Proceedings of the National Academy of Sciences, 1994. 91(14): p. 6604-6608.
19. Laidler, K.J., *The development of the Arrhenius equation.* Journal of Chemical Education, 1984. 61(6): p. 494.
20. Geerlings, P., F. De Proft, and W. Langenaeker, *Conceptual Density Functional Theory.* Chemical Reviews, 2003. 103(5): p. 1793-1874.
21. Parr, R.G. and W. Yang, *Density functional approach to the frontier-electron theory of chemical reactivity.* Journal of the American Chemical Society, 1984. 106(14): p. 4049-4050.
22. Osorio, E., et al., *Why is quercetin a better antioxidant than taxifolin? Theoretical study of mechanisms involving activated forms.* Journal of Molecular Modeling, 2013. 19(5): p. 2165-2172.
23. Fuentealba, P., E. Florez, and W. Tiznado, *Topological Analysis of the Fukui Function.* Journal of Chemical Theory and Computation, 2010. 6(5): p. 1470-1478.
24. Tiznado, W., et al., *Comparison among Four Different Ways to Condense the Fukui Function.* The Journal of Physical Chemistry A, 2005. 109(14): p. 3220-3224.
25. Chattaraj, P.K., B. Maiti, and U. Sarkar, *Philicity: A Unified Treatment of Chemical Reactivity and Selectivity.* The Journal of Physical Chemistry A, 2003. 107(25): p. 4973-4975.
26. Lee, C., W. Yang, and R.G. Parr, *Development of the Colle-Salvetti correlation-energy formula into a functional of the electron density.* Physical Review B, 1988. 37(2): p. 785-789.
27. Becke, A.D., *Density‐functional thermochemistry. III. The role of exact exchange.* The Journal of Chemical Physics, 1993. 98(7): p. 5648-5652.
28. McLean, A.D. and G.S. Chandler, *Contracted Gaussian basis sets for molecular calculations. I. Second row atoms, Z=11–18.* The Journal of Chemical Physics, 1980. 72(10): p. 5639-5648.
29. Krishnan, R., et al., *Self‐consistent molecular orbital methods. XX. A basis set for correlated wave functions.* The Journal of Chemical Physics, 1980. 72(1): p. 650-654.
30. Frisch, M.J., et al., *Gaussian 09*. 2009, Gaussian, Inc.: Wallingford, CT, USA.
31. Kohn, W. and L.J. Sham, *Self-Consistent Equations Including Exchange and Correlation Effects.* Physical Review, 1965. 140(4A): p. A1133-A1138.
32. Marenich, A.V., C.J. Cramer, and D.G. Truhlar, *Universal Solvation Model Based on Solute Electron Density and on a Continuum Model of the Solvent*

Defined by the Bulk Dielectric Constant and Atomic Surface Tensions. The Journal of Physical Chemistry B, 2009. 113(18): p. 6378-6396.

33. Hratchian, H.P. and H.B. Schlegel, *Accurate reaction paths using a Hessian based predictor–corrector integrator.* The Journal of Chemical Physics, 2004. 120(21): p. 9918-9924.
34. Pham, A.L.-T., F.M. Doyle, and D.L. Sedlak, *Kinetics and efficiency of H2O2 activation by iron-containing minerals and aquifer materials.* Water Research, 2012. 46(19): p. 6454-6462.
35. Zazo, J.A., et al., *Chemical Pathway and Kinetics of Phenol Oxidation by Fenton's Reagent.* Environmental Science & Technology, 2005. 39(23): p. 9295-9302.
36. Atoguchi, T., et al., *Phenol oxidation into catechol and hydroquinone over H-MFI, H-MOR, H-USY and H-BEA in the presence of ketone.* Journal of Molecular Catalysis A: Chemical, 2004. 220(2): p. 183-187.
37. Youmin, S., et al., *The degradation mechanism of phenol induced by ozone in wastes system.* Journal of Molecular Modeling, 2012. 18(8): p. 3821-3830.
38. Radeglia, R., *Reichardt, C.: Solvent Effects in Organic Chemistry. 1. Aufl., XI, 355 S., 45 Abb., 69 Tab., Format 17×24,3 cm. Weinheim-New York: Verlag Chemie 1979. (Monographs in Modern Chemistry, Vol. 3). Leinen DM 108,–.* Journal für Praktische Chemie, 1981. 323(6): p. 1015-1016.
39. Russell, G.A., *Solvent Effects in the Reactions of Free Radicals and Atoms. IV. Effect of Aromatic Solvents in Sulfuryl Chloride Chlorinations1.* Journal of the American Chemical Society, 1958. 80(18): p. 5002-5003.
40. Horn, M. and K. Matyjaszewski, *Solvent Effects on the Activation Rate Constant in Atom Transfer Radical Polymerization.* Macromolecules, 2013. 46(9): p. 3350-3357.
41. Kim, J., D.S. Clark, and J.S. Dordick, *Intrinsic effects of solvent polarity on enzymic activation energies.* Biotechnology and Bioengineering, 2000. 67(1): p. 112-116.
42. Jen, J.-F., M.-F. Leu, and T.C. Yang, *Determination of hydroxyl radicals in an advanced oxidation process with salicylic acid trapping and liquid chromatography.* Journal of Chromatography A, 1998. 796(2): p. 283-288.
43. Buxton, G.V., et al., *Critical Review of rate constants for reactions of hydrated electrons, hydrogen atoms and hydroxyl radicals (·OH/·O− in Aqueous Solution.* Journal of Physical and Chemical Reference Data, 1988. 17(2): p. 513-886.